Tuijin Jishu/Journal of Propulsion Technology
ISSN: 1001-4055
Vol. 45 No. 4 (2024)

Onset of Magneto - Convective Instability of a Casson Nanofluid with Helical Force: Linear and Weakly Non-Linear Analyses

K Narayana Chary[1], N. Kishan[1], J. SharathKumar Reddy[2]

[1]*Department of Mathematics, University College of Science, Osmania University, Hyderabad, Telangana,500007, India.*

[2]*Department of Mathematics, Anurag University, Hyderabad, Telangana, India.*

Abstract: - The study investigates the thermal convection of a Casson nanofluid in a horizontal layer influenced by magnetic and helical force parameters. Both linear and weakly non-linear analyses are performed to assess the fluid's stability. The critical Rayleigh number is calculated in the linear analysis, while the Nusselt number is determined in the weakly non-linear analysis which is used to study heat transfer. A one-term Galerkin approach is employed to study the linear theory, while multiple scale analysis is used to investigate the weakly non-linear theory. The Hartman number (Ha^2) exerts a stabilizing effect on the system in both stationary and oscillatory convection. Meanwhile, the helical force parameter (S_h), the adjusted diffusivity ratio (Na) and the nanoparticle Rayleigh number (Rn) have a destabilizing effect on the system in both stationary and oscillatory convection. The Lewis number (Le) and Prandtl number (Pr) exhibit a stabilizing effect on oscillatory convection, but in the case of stationary convection, they do not have any impact on the system. The Casson parameter (β) has a destabilizing effect in the case of stationary convection, whereas it shows a stabilizing effect on the system in oscillatory convection.

Keywords*: Casson nano fluid, Linear stability analysis, Thermal convection*.

1. Introduction

In recent times, there has been a surge in the exploration of nanofluids, a novel blend comprising regular fluids and minute suspended nanoparticles. Coined as 'Nanofluid' by Choi [6], these fluids exhibit enhanced heat transfer capabilities compared to conventional fluids, rendering them invaluable across a multitude of applications spanning various fields. Buongiorno [3] made a noteworthy advancement in nanofluid modeling by highlighting the significant influence of both the base fluid velocity and relative velocity on the absolute velocity of nanoparticles. This model has been widely adopted by researchers [22], [23], [24], [16], [5], [18] to investigate convective heat transfer in nanofluids, and it was subsequently refined by Nield and Kuznetsov [15] to incorporate solutal effects on nanofluid layers. The Casson model has demonstrated excellent compatibility with diverse non-Newtonian fluids [7]. Blair and Spanner [19] observed that the properties of blood closely align with those of a Casson fluid in moderate shear rate flows, thus justifying the utilization of the Casson model for blood flow. Scott Blair [20] investigated the efficacy of Casson's equation, while Hamid et al. [11] uncovered dual nature solutions for the proposed model, incorporating thermal radiation effects on both steady and unsteady Casson fluid flows. Aneja et al. [2] explored natural instability in a partially heated porous medium using a penalty finite element approach for Casson fluid. Recently, researchers have applied the Casson model to various nanofluid flow problems to examine the influence of nanoparticles on blood flow.

In recent years, nanoparticles have emerged as highly versatile tools in the treatment of numerous ailments. Gold nanoparticles, in particular, are utilized in cancer therapy due to their larger size and remarkable energy absorption capabilities. Moreover, nanoparticles influence the efficiency of heat transfer mechanisms, particularly convection, between the heart and the body's surface through the bloodstream. Consequently, the convective

instability of blood in the presence of nanoparticles plays a pivotal role in advancing medical practices and enhancing healthcare outcomes. Gupta et al. [9] previously explored convection currents within Casson nanofluids incorporating internal heating effects. More recently, Gupta et al. [10] conducted an analytical and numerical investigation into the binary instability of Casson nanofluids. Phenomena of linear and weakly nonlinear thermal convection within Casson nanofluids subjected to helical force and magnetic effects [8], [17]. The structure of the paper is outlined as follows: Section 2 elaborates on the governing equations, while Sections 3 and 4 delve into the linear and weakly nonlinear theories, respectively. Subsequently, Sections 5 and 6 present the findings of the analysis, followed by a conclusion and discussion of the results.

2. Mathematical formulation:

The rheological equation of Casson fluid flow [21], [1], [12], [14], [13], [4] is,

$$\tau_{ij} = \mu_B + (\frac{P_y}{\sqrt{2\pi}})2e_{ij}, \pi > \pi_c, \tag{1}$$

$$\tau_{ij} = \mu_B + (\frac{P_y}{\sqrt{2\pi_c}})2e_{ij}, \pi < \pi_c. \tag{2}$$

where,

$$\begin{cases} \mu_B = \ dynamic\ viscosity, e_{ij} = \ deformation\ rate, \\ \pi_c = \ critical\ value\ of\ \pi = e_{ij}e_{ij}\ \left(where\ e_{ij}\ is\ the\ (i,j)th\ segment\ of\ deforming\ rate\right), \\ P_y = \ yield\ stress\ below\ which\ there\ is\ no\ flow\ occurs\ and\ \tau\ is\ the\ stress\ tensor\ for\ Casson\ fluid. \end{cases}$$

Now we have to consider a layer of Casson nanofluid confined between the planes $z^* = 0$ and $z^* = d$ under a small temperature gradient $(T_0^* - T_1^*), T_0^* > T_1^*$ and uniform internal heat source Q_0. Let us assume a frame in which the z^*-axis is adjusted vertically upward. The asterisk was used to explicit dimensional variables. The incompressible governing equations for fluid glide with the idea that agglomeration of debris does no longer occur and the suspension remains strong [21], [1] are,

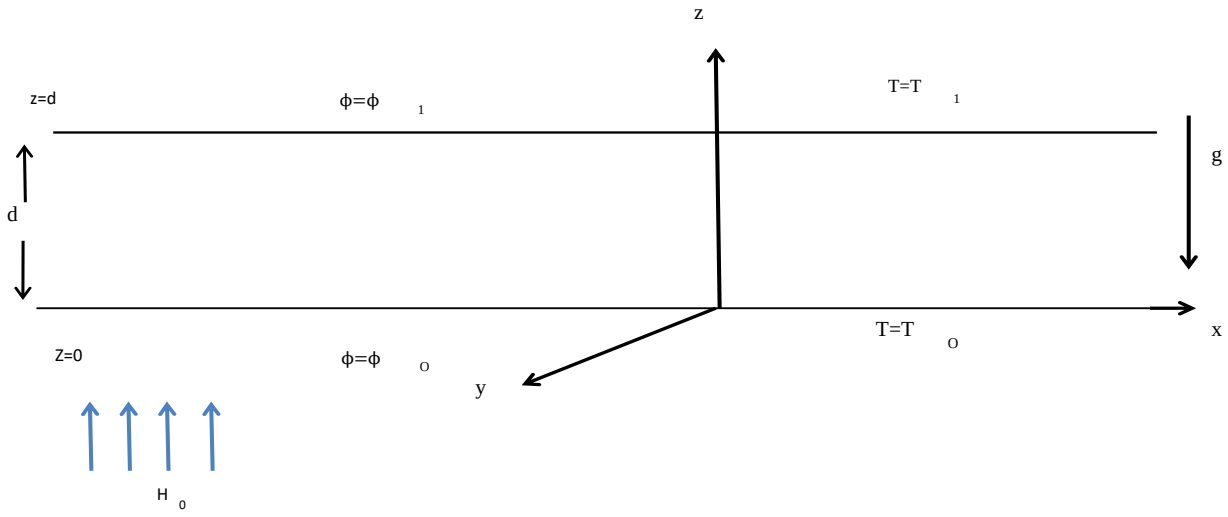

Figure 1: Physical Diagram

Continuity equation: $$\nabla^* \cdot v^* = 0. \tag{3}$$

Momentum equation: $$\rho(\frac{\partial}{\partial t^*} + v^* \cdot \nabla^*)v^* = -\nabla^* p^* + div\tau + [\phi^* \rho_p + (1-\phi^*)(1-\beta(T^* - T_0^*))]g$$
$$+\sigma_1(V \times B_0\hat{e}_z) \times B_0\hat{e}_z + \rho_0 a\Omega df. \tag{4}$$

Using Eq.(3) in Eq. (4), we get,

$$\rho_{f0}[\frac{\partial v^*}{\partial t^*} + v^* \cdot \nabla^* v^*) = -\nabla^* p^* + (1 + \frac{1}{\beta})\mu\nabla^{*2} v^* + [\phi^* \rho_p + (1 - \phi^*)(1 - \beta(T^* - T_0^*))]g$$

$$+\sigma_1(V \times B_0 \hat{e}_z) \times B_0 \hat{e}_z + \rho_0 a\Omega df. \quad (5)$$

There is no buoyancy term present in the x and y axes and the Boussinesq approximation was used. The left hand side of Eq. (5) indicates the inertial term, the right hand side offers the strain gradient and lastly the viscous time period.

The equation of nanoparticles changes when there is no chemical reaction,

$$\frac{\partial \phi^*}{\partial t^*} + v^* \cdot \nabla\phi^* = -\frac{1}{\rho_p}\nabla \cdot j_p. \quad (6)$$

Here diffusion mass flux of nanoparticles j_p is the sum of two diffusion terms given as,

$$j_p = j_{p,b} + j_{p,t} = -\rho_p D_b \nabla\phi^* - \rho_p D_t \frac{\nabla T^*}{T_0^*}. \quad (7)$$

Combining Eqs. (5) and (6), we get,

$$\frac{\partial \phi^*}{\partial t^*} + v^* \cdot \nabla\phi^* = D_b \nabla^{*2}\phi^* + (\frac{D_t}{T_0^*})\nabla^{*2} T^*. \quad (8)$$

Equation of energy,

$$(\rho c)_f[\frac{\partial T^*}{\partial t^*} + v^* \cdot \nabla T^*] = k\nabla^{*2} T^* + (\rho c)_p[D_b \nabla^* \phi^* \cdot \nabla^* T^* + \frac{D_t}{T_0^*}\nabla^* T^* \cdot \nabla^* T^*]. \quad (9)$$

By using nano-outcomes (Brownian diffusion and thermophoresis), equation (8) balances the terms for convection and conduction in the presence of nanoparticles and an internal heat source.

$$\begin{cases} v^* = (u^*, v^*, w^*) = Velocity, \quad t^* = Time, \quad p^* = Pressure, \\ \beta = \mu_B \dfrac{\sqrt{2\pi}}{P_y} = \ The\ \ Casson\ \ fluid\ \ parameter, \\ \phi^* = The\ \ particle\ \ volume\ \ fraction, \quad T^* = The\ temperature, \\ \mu = The\ \ fluid\ \ viscosity, \\ g = \ The\ \ acceleration\ \ due\ \ to\ \ gravity, \\ k = The\ \ effective\ \ thermal\ \ conductivity\ \ of\ \ the\ nanofluid, \rho = \ The\ \ density, \\ \rho c = \ The\ \ heat\ \ capacity, Q_0 = \ Volumetricheat\ \ source. \\ D_b = Diffusion\ coefficientof\ \ Brownian, D_t = \ \ thermophoresis\ \ diffusion\ \ coefficient \end{cases}$$

Assuming that the nanoparticles' volumetric fraction and temperature are constant at the initial stage,

$$T^* = T_0^*, \phi^* = \phi_0^* \ \ at\ \ Z^* = 0, \quad (10)$$

$$T^* = T_1^*, \phi^* = \phi_1^* \ \ at\ \ Z^* = d. \quad (11)$$

At the basic state, we anticipate that the fluid layer is relaxed and the fraction of nanoparticles is constant, while the other variables primarily fluctuate along the horizontal axis.

The basic state of the Casson nano fluid is described by,

$$v_b = 0,\ \phi_b = 0,\ T_b = T_0 - \left(\frac{\Delta T}{d}\right) z. \quad (12)$$

The non-dimensional parameters are,

$$\begin{cases} (x,y,z)=(\frac{x^*}{d},\frac{y^*}{d},\frac{z^*}{d}); & t=\frac{T^*\alpha_f}{d2}; \\ (u,y,z)=(\frac{u^*d}{\alpha_f},\frac{v^*}{\alpha_f},\frac{v^*}{\alpha_f}); & \alpha_f=\frac{k}{(\rho c_p)_f}. \\ \phi=\frac{(\phi^*-\phi_0^*)}{(\phi_1^*-\phi_0^*)}; & T=\frac{(T^*-T_1^*)}{T_0^*-T_1^*}; \\ p=\frac{p^*K2}{\mu\alpha_f}; & \end{cases}$$

So far, it has been assumed that the spatial variations of k and μ are negligible. Indices "p", "f" and "0" seek advice from particles, fluids or reference variables. Then the Eqs. (3),(5),(8) and (9) Reduce,

$$\nabla\cdot v=0, \tag{13}$$

$$\frac{1}{Pr}(\frac{\partial v}{\partial t}+v\cdot\nabla v)=-\nabla p+(1+\frac{1}{\beta})\nabla^2 v-Rme_z+RaTe_z-Rn\phi e_z+S_h f+Ha^2[(V'\times\hat{e}_z)\times\hat{e}_z] \tag{14}$$

$$\frac{\partial T}{\partial t}+v\cdot\nabla T=w+\nabla^2 T+\frac{Nb}{Le}\nabla\phi.\nabla T+\frac{NaNb}{Le}\nabla T\cdot\nabla T, \tag{15}$$

$$\frac{\partial\phi}{\partial t}+v\cdot\nabla\phi=\frac{1}{Le}\nabla^2\phi+\frac{Na}{Le}\nabla^2 T. \tag{16}$$

The boundary conditions in Eqs. (10) and (11) in the form of non-dimensional terms,

$$w=0,\ D^2w=0,\ \phi=0,\ T=0\ at\ Z=0, \tag{17}$$

$$w=0,\ D^2w=0,\phi=0,\ T=0\ at\ Z=1. \tag{18}$$

$$\begin{cases} Ra=\rho_{f0}gK^3\beta_1\frac{(T_0^*-T_1^*)}{\mu\alpha_f}(\ Rayleigh\ number\ );Le=\frac{\alpha_f}{D_b}(\ Lewis\ number\ ); \\ Pr=\frac{\mu}{\rho\alpha_f}(\ Prandtl\ number\ ),Ha=B_0L\sqrt{\frac{\sigma_1}{\mu}}(\ Hartmann\ number\ ). \\ Nb=(\rho c)_p\frac{(\phi_0^*-\phi_1^*)}{\rho c}(\ Particle\ density\ increment\ ), \\ Na=\frac{D_t}{D_b}\frac{(T_0^*-T_1^*)}{T_1(\phi_1^*-\phi_0^*)}(\ Adjusted\ diffusivity\ proportion\ (modified\ diffusivity\ ratio)\ ), \\ Rm=(\frac{\rho_p\phi_0^*+\rho_{f0}(1-\phi_0^*)}{\mu\alpha_f})gK^3(\ Thermal\ Rayleigh\ number\ ), \\ Rn=\frac{(\rho_p-\rho_{f0})(\phi_1^*-\phi_0^*)}{\mu\alpha_f}gK^3(\ Nanoparticle\ Rayleigh\ number\ ), \\ S_h=\frac{a\Omega d^2}{\nu}\ (Helical\ force\ parameter). \end{cases}$$

To explore linear theory, consider the linear part of eqs. (13)-(16),

$$\frac{1}{p_r}\frac{\partial v}{\partial t}=-\nabla p+(1+\frac{1}{\beta})\nabla^2 v-Rme_z+RaTe_z-Rn\phi e_z+Ha^2[(V'\times\hat{e}_z)\times\hat{e}_z]+S_h f, \tag{19}$$

$$\frac{\partial T}{\partial t}=w+\nabla^2 T, \tag{20}$$

$$\frac{\partial\phi}{\partial t}=\frac{1}{Le}\nabla^2\phi+\frac{Na}{Le}\nabla^2 T, \tag{21}$$

$$w=0,D^2w=0,\phi=0,T=0\ at\ Z=0,$$

$$w=0,D^2w=0,\phi=0,T=0\ at\ Z=1. \tag{22}$$

By Taking the third components of curl of Eq.(19) and curl of curl of Eq. (19), we obtain,

$$\left(\frac{1}{Pr}\frac{\partial}{\partial t}-(1+\frac{1}{\beta})\nabla^2+Ha^2\right)w_z-S_h\frac{\partial^2 w}{\partial z^2}=0, \tag{23}$$

$$\left(\frac{1}{Pr}\frac{\partial}{\partial t}-(1+\frac{1}{\beta})\nabla^2+Ha^2\frac{\partial^2}{\partial z^2}\right)\nabla^2 w+(Rn\phi-RaT)\nabla_h^2-S_h\left(\nabla_h^2 w_z-\frac{\partial^2 w_z}{\partial z^2}\right)=0 \tag{24}$$

where $\omega_z=(\nabla\times V)\cdot\hat{e}_z$, $\nabla_h^2=\frac{\partial^2}{\partial x^2}+\frac{\partial^2}{\partial y^2}$, and $\nabla^2=\frac{\partial^2}{\partial x^2}+\frac{\partial^2}{\partial y^2}+\frac{\partial^2}{\partial z^2}$.

Now Eqs. (23), (24), (20) and (21) becomes,

$$A_1 w_z-S_h\frac{\partial^2 w}{\partial z^2}=0, \tag{25}$$

$$A_2 w-S_h\left(\nabla_h^2 w_z-\frac{\partial^2 w_z}{\partial z^2}\right)+(Rn\phi-RaT)\nabla_h^2=0, \tag{26}$$

$$A_3 T-w=0, \tag{27}$$

$$A_4\phi=\frac{Na}{Le}\nabla^2 T. \tag{28}$$

Where,

$$\begin{cases} A_1=\left(\frac{1}{Pr}\frac{\partial}{\partial t}-(1+\frac{1}{\beta})\nabla^2+Ha^2\right), \\ A_2=\left(\frac{1}{Pr}\frac{\partial}{\partial t}\nabla^2-(1+\frac{1}{\beta})\nabla^4+Ha^2\frac{\partial^2}{\partial z^2}\right) \\ A_3=\frac{\partial}{\partial t}-\nabla^2, \\ A_4=\frac{\partial}{\partial t}-\frac{1}{Le}\nabla^2. \end{cases}$$

Let us replace $w=\sin\pi z e^{i(lx+my)+\sigma t}$, where $\sigma=iw$ in (25)-(28) then we have obtained,

$$Ra=\frac{X_1+X_2\omega^2+X_3\omega^4+X_4\omega^6+i(X_4\omega+X_5\omega^3+X_7\omega^5)}{X_8+X_9\omega^2+X_{10}\omega^4}. \tag{29}$$

Where,

$$X_1=Pr^4\beta\delta^4(Ha^2\beta+(1+\beta)\delta^2)((Ha^2\beta+(1+\beta)\delta^2)(-Naq^2Rn\beta+Ha^2\beta\delta^2\pi^2+(1+\beta)\delta^6)+(-\pi^2+q^2)\beta^2\delta^2{S_h}^2)\pi^2,$$

$$X_2=Pr^2\beta\delta^2(Ha^6Le^2\pi^2Pr^2\beta^3-Naq^2Rn\beta^3\delta^2+(1+\beta)(Le^2Pr^2(1+\beta)^2-\beta(Pr+(-1+Pr)\beta))\delta^8+Ha^4Pr\beta^2\delta^2(-\beta\delta^2+Le^2Pr(1+\beta)(2\pi^2+\delta^2))+Ha^2\beta\delta^4(Le^2Pr^2(1+\beta)^2(\pi^2+2\delta^2)+\beta(\pi^2\beta-2Pr(1+\beta)\delta^2))-\pi^2Pr(\pi-q)(\pi+q)\beta^2(Ha^2Le^2Pr\beta+(\beta+Le^2Pr(1+\beta))\delta^2)S_h^2),$$

$$X_3=-Pr\beta^2(Ha^2Le^2Pr(-\pi^2+Ha^2pr)\beta^2\delta^2+2Ha^2Le^2Pr^2\beta(1+\beta)\delta^4+(\beta^2+Le^2Pr(1+\beta)(Pr+(-1+Pr)\beta))\delta^6+Le^2\pi^2Pr^2(\pi-q)(\pi+q)\beta^2S_h^2),$$

$$X_4=-Le^2Pr\beta^4\delta^2,$$

$$X_5=Pr^3\beta\delta^2((Ha^2\beta+(1+\beta)\delta^2)^2(LeNaPrq^2Rn\beta+Ha^2\pi^2Pr\beta\delta^2+(Pr+\beta+Pr\beta)\delta^6)-\pi^2(\pi-q)(\pi+q)\beta^2\delta^2(Ha^2Pr\beta+(Pr+(-1+Pr)\beta)\delta^2)S_h^2),$$

$$X_6=Pr\beta(Ha^6Le^2\pi^2Pr^3\beta^3+LeNaPrq^2Rn\beta^3\delta^2+(Pr+\beta+Pr\beta)(\beta^2+Le^2Pr^2(1+\beta)^2)\delta^8+Ha^4Le^2Pr^2\beta^2\delta^2(2\pi^2Pr(1+\beta)+(Pr+\beta+Pr\beta)\delta^2)+Ha^2Pr\delta^4(\pi^2\beta^3+Le^2Pr\beta(1+\beta)(\pi^2Pr(1+\beta)+2(Pr+\beta+Pr\beta)\delta^2))-Le^2\pi^2Pr^2(\pi-q)(\pi+q)\beta^2(Ha^2pr\beta+(Pr+(-1+Pr)\beta)\delta^2)S_h^2),$$

$X_7 = Le^2 Pr\beta^3(Ha^2\pi^2 Pr\beta + (Pr + \beta + Pr\beta)\delta^4)$,

$X_8 = Pr^4 q^2\beta^2\delta^4(Ha^2\beta + (1+\beta)\delta^2)^2$,

$X_9 = Pr^2 q^2\beta^2(Ha^4 Le^2 Pr^2\beta^2 + 2Ha^2 Le^2 Pr^2\beta(1+\beta)\delta^2 + (\beta^2 + Le^2 Pr^2(1+\beta)^2)\delta^4)$,

$X_{10} = Le^2 Pr^2 q^2\beta^4$. (30)

3. Stationary Convection

First, we consider stationary instability, i.e., $\omega = 0$ is real. The stationary Rayleigh number Ra_{sc} can be written as,

$$Ra_{sc} = -NaRn + \frac{Ha^2\pi^2\delta^2}{q^2} + \frac{(1+\frac{1}{\beta})\delta^6}{q^2} + \frac{\pi^2(-\pi^2+q^2)\delta^2 S_h^2}{q^2(Ha^2+(1+\frac{1}{\beta}\delta^2))}. \quad (31)$$

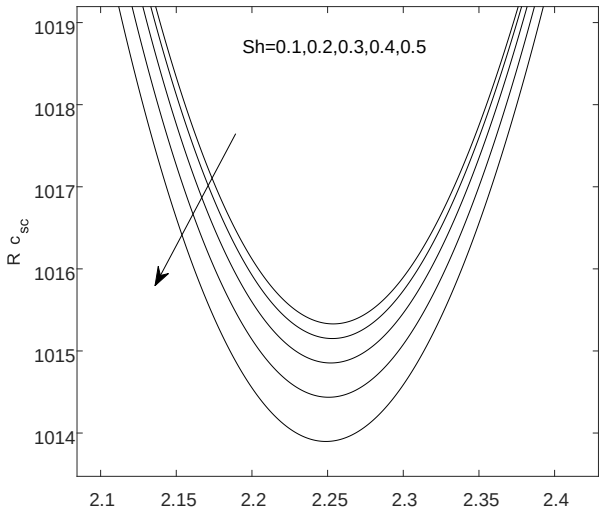

Figure 2: Neutral stability curves for Ra_{sc} with different values of Sh for fixed values of $Le = 5$, $Pr = 5$, $Ha^2 = 0.2$, $Na = 1$, $\beta = 2$ and $Sh = 0.1$.

4. Oscillatory Convection

We considered the real and imaginary components of Ra, requiring the imaginary part of Ra to vanish. This condition allows us to solve for ω^2. By substituting ω^2 back into the real part of Ra, we derive the thermal Rayleigh number for oscillatory convection, denoted as Ra_{oc}.

$$Ra_{oc} = \frac{X_1 + X_2\omega^2 + X_3\omega^4 + X_4\omega^6}{X_8 + X_9\omega^2 + X_{10}\omega^4}. \quad (32)$$

Where , $\omega^2 = \frac{-X_6 \pm \sqrt{(X_6{}^2 - 4X_7X_5)}}{2X_7}$.

From this, we obtain two roots. If one root is positive and the other is negative, we select the positive root. If both roots are positive, we choose the smaller of the two.

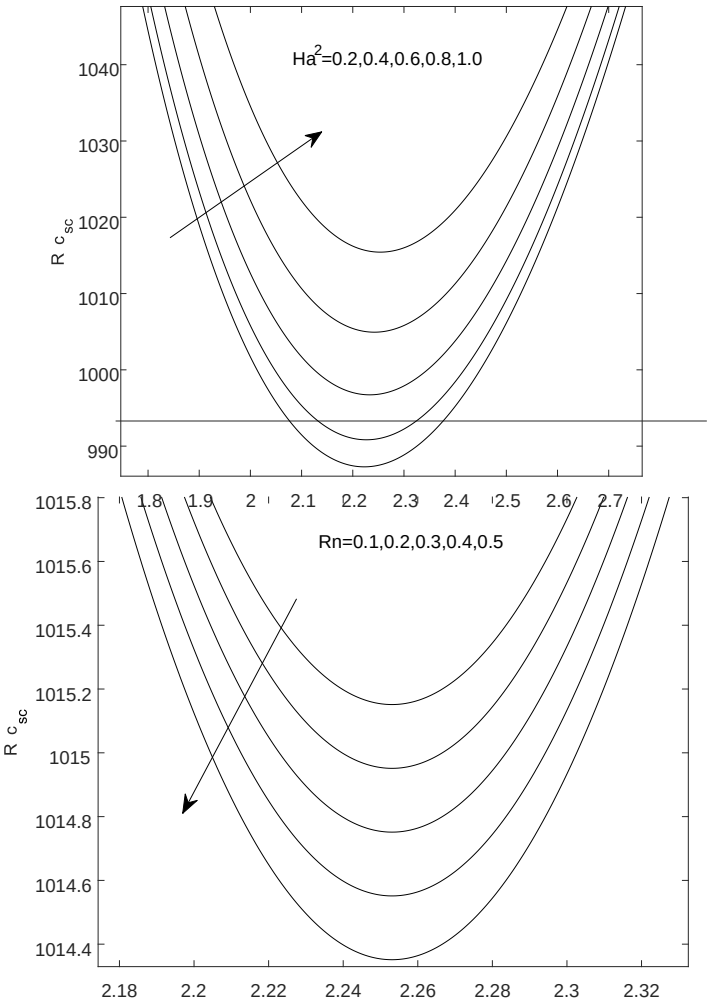

Figure 3:Neutral stability curves for Ra_{sc} with different values of Rn for fixed values of $Le = 5$, $Pr = 5$, $Na = 2$, $\beta = 2$, $Ha^2 = 1$ and $S_h = 0.2$.

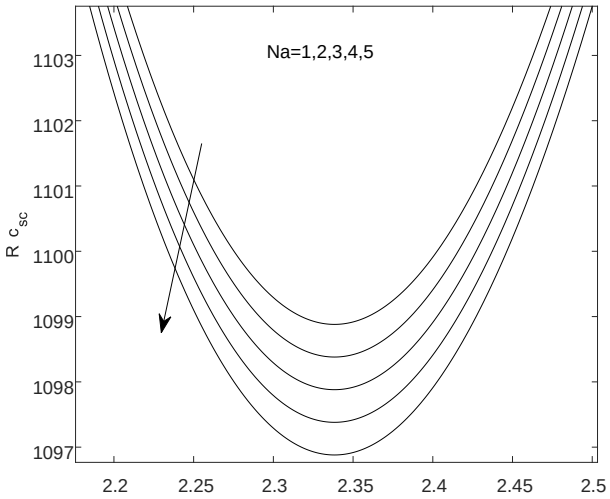

Figure 4:Neutral stability curves for Ra_{sc} with different values of Na for fixed values of $Le = 5$, $Pr = 5$, $Ha^2 = 2$,$\beta = 2$, $Rn = 0.5$ and $S_h = 0.5$

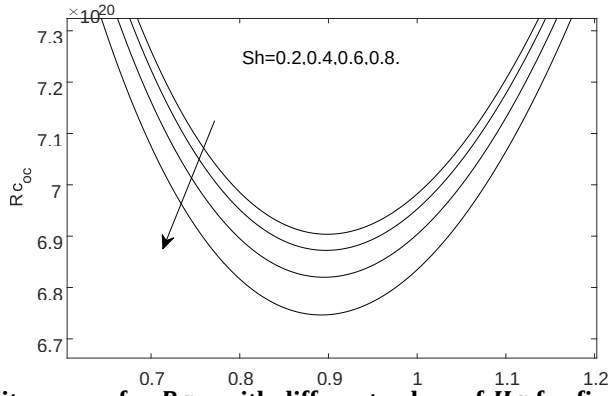

Figure 5:Neutral stability curves for Ra_{sc} with different values of Ha for fixed values of $Le = 5$, $Pr = 5$, $Na = 1$,$Rn = 0.1$,$\beta = 2$ and $S_h = 0.1$.

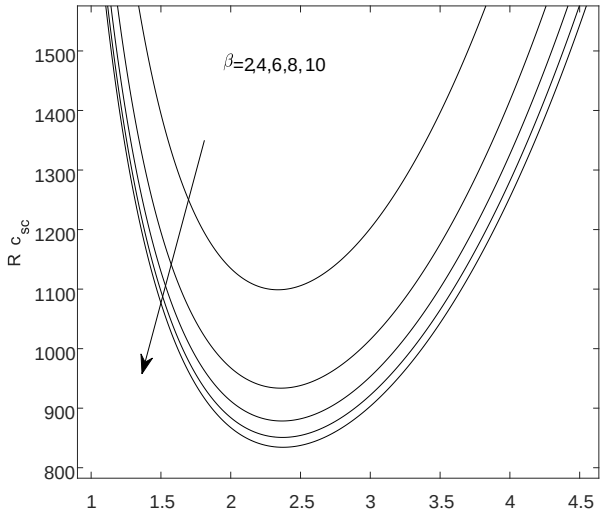

Figure 6:Neutral stability curves for Ra_{sc} with different values of β for fixed values of $Le = 5$, $Rn = 0.5$, $Pr = 5$, $Na = 1$,, $Ha^2 = 2$, and $S_h = 0.5$.

Figure 7:Neutral stability curves for Ra_{oc} with different values of sh for fixed values of $Rn = 0.1$, $Pr = 10$, $Na = 1$,$\beta = 5$, $Le = 5$and $Ha^2 = 1$.

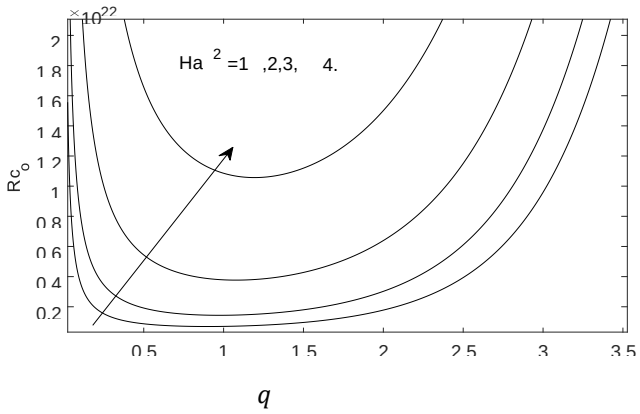

Figure 8:Neutral stability curves for Ra_{oc} with different values of Ha^2 for fixed values of $Rn = 0.1$, $Pr = 10$, $Na = 1$, $\beta = 5$, $Le = 5$and $S_h = 0.2$.

q

Figure 9:Neutral stability curves for Ra_{oc} with different values of Na for fixed values of $Rn = 1$, $Pr = 2$, $S_h = 2$, $\beta = 5$, $Le = 5$ and $Ha^2 = 1$.

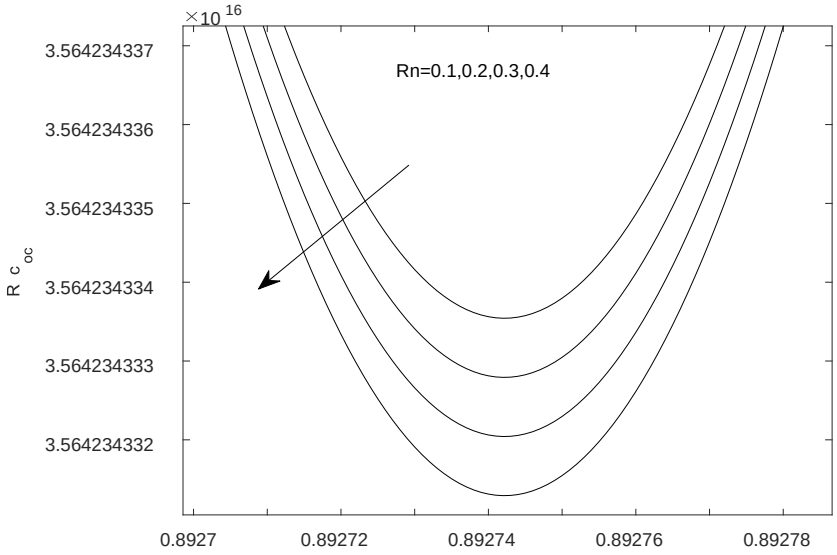

q

Figure 10:Neutral stability curves for Ra_{oc} with different values of Rn for fixed values of $Rn = 0.1$, $Pr = 5$, $Na = 1$, $\beta = 2$, $S_h = 0.2$ $Le = 5$ and $Ha^2 = 1$.

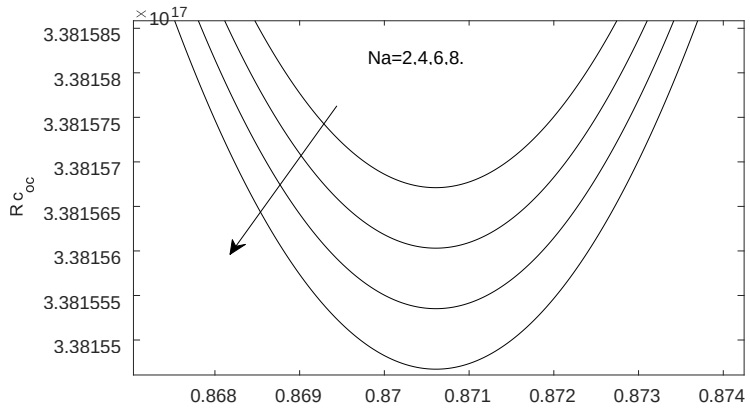

Figure 11:Neutral stability curves for Ra_{oc} with different values of β for fixed values of $Rn = 0.1$, $Pr = 2$, $Na = 1$, $\beta = 2$, $S_h = 2$ $Le = 2$ and $Ha^2 = 0.2$.

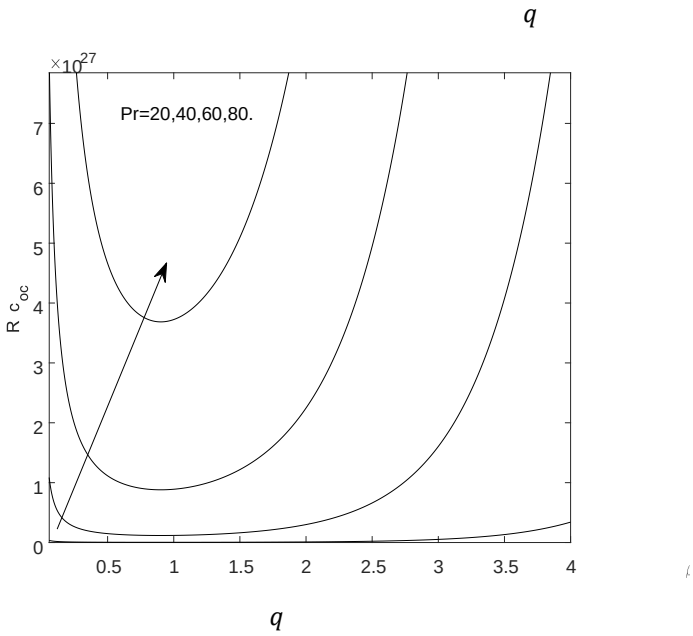

Figure 12:Neutral stability curves for Ra_{oc} with different values of Pr for fixed values of $Rn = 0.1$, $Pr = 2$, $Na = 1$, $\beta = 10$, $S_h = 0.2$ $Le = 5$ and $Ha^2 = 1$.

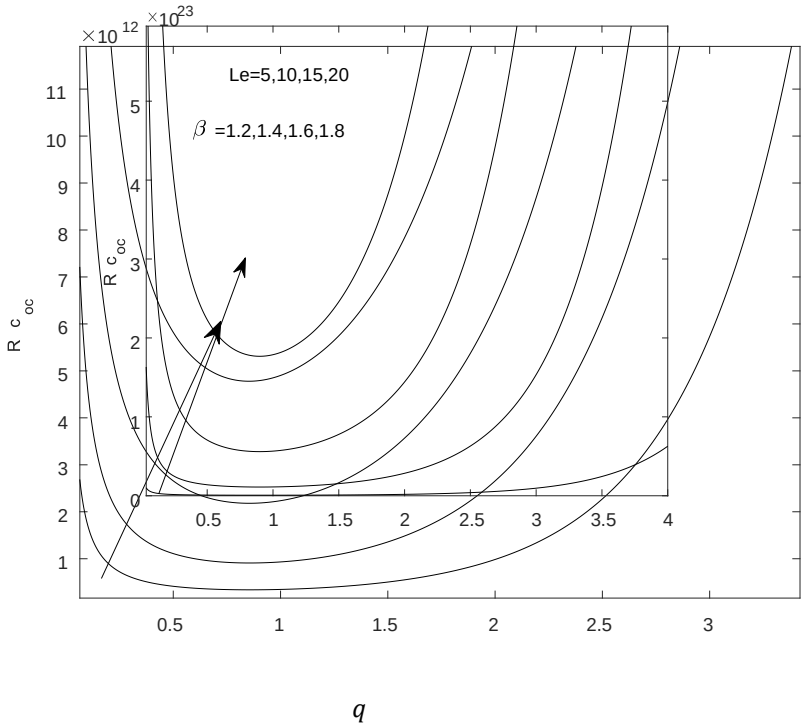

Figure 13:Neutral stability curves for Ra_{oc} with different values of Le for fixed values of $Rn = 0.1$, $Pr = 10$, $Na = 1$, $\beta = 5$, $S_h = 0.2$ $Le = 2$ and $Ha^2 = 1$.

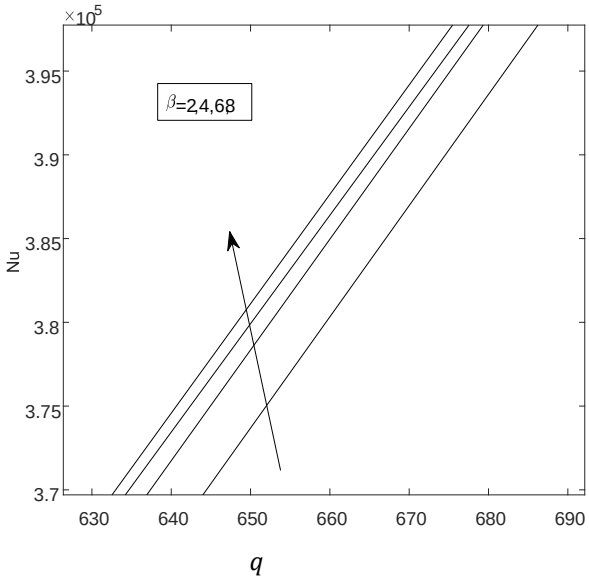

Figure 14:The change of Nu vs Rsc,with different values of β for fixed vales of $Le = 0.5$, $Pr = 0.1$, $Rn = 0.2$, $S_h = 5$, $Ha^2 = 0.1$ and $Na = 0.2$.

5. Weakly nonlinear analysis

To investigate the type of convective motion, weakly nonlinear theory is needed. We consider the non-dimensional equations with non linear terms, which are,

$$\frac{1}{Pr}\left(\frac{\partial v}{\partial t} + (v.\nabla)v\right) = -\nabla p + (1 + \frac{1}{\beta})\nabla^2 v - Rme_z + RaTe_z - Rn\phi e_z - S_h\, f + Ha^2[(V' \times \hat{e}_z) \times \hat{e}_z], \tag{33}$$

$$\frac{\partial T}{\partial t} + (v.\nabla)T = w + \nabla^2 T + \frac{NaNb}{Le}\nabla T.\nabla T + \frac{Nb}{Le}\nabla T.\nabla\phi, \tag{34}$$

$$\frac{\partial \phi}{\partial t} + (v.\nabla)\phi = \frac{1}{Le}\nabla^2\phi + \frac{Na}{Le}\nabla^2 T. \tag{35}$$

To study the weakly nonlinear theory, we follow the multiple scale analysis. We write the governing equations as follows(after eliminating T and ϕ),

$$Lw = N. \tag{36}$$

Where,

$$\begin{cases} L = & A_1A_2A_3A_4 - S_h^2\dfrac{\partial^2}{\partial z^2}\left(\nabla_h^2 - \dfrac{\partial^2}{\partial z^2}\right)A_3A_4 - A_1A_4\nabla_h^2 Ra + \dfrac{Na}{Le}\nabla_h^2\nabla^2 RnA_1, \\ N = & A_3A_4N_1S_h^2\left(\nabla_h^2 - \dfrac{\partial^2}{\partial z^2}\right) - \left(A_1\nabla_h^2 Rn\dfrac{Na}{Le}\nabla^2\right)(N_3 + N_4 + N_5) - N_6A_1A_3\nabla_h^2 Rn + + \\ & + A_1A_3A_4N_2 + A_1A_4\nabla_h^2 Ra(N_3 + N_4 + N_5). \end{cases}$$

Where,

$$\begin{cases} N_1 = -\frac{1}{Pr}\nabla \times (v \cdot \nabla)v, \\ N_2 = -\frac{1}{Pr}\nabla \times (\nabla \times (v \cdot \nabla)v), \\ N_3 = \frac{Nb}{Le}\nabla\phi \cdot \nabla T, \\ N_4 = \frac{NaNb}{Le}\nabla T \cdot \nabla T, \\ N_5 = -v \cdot \nabla T, \\ N_6 = -v \cdot \nabla\phi. \end{cases}$$

We write u, v, w, T and ϕ in the series expansion interms of ϵ,

$$u = \epsilon u_0 + \epsilon^2 u_1 + \epsilon^3 u_2 + \cdots,$$
$$v = \epsilon v_0 + \epsilon^2 v_1 + \epsilon^3 v_2 + \cdots,$$
$$w = \epsilon w_0 + \epsilon^2 w_1 + \epsilon^3 w_2 + \cdots,$$
$$T = \epsilon T_0 + \epsilon^2 T_1 + \epsilon^3 T_2 + \cdots,$$
$$\phi = \epsilon \phi_0 + \epsilon^2 \phi_1 + \epsilon^3 \phi_2 + \cdots. \quad (37)$$

Where, $\epsilon^2 = \frac{Ra - Ra_{sc}}{Ra_{sc}} << 1.$

The first approximations are,

$$u_0 = \frac{i\pi}{q_{sc}}\left[Ae^{iq_{sc}x}\cos\pi z - c.c\right],$$
$$w_0 = \left[Ae^{iq_{sc}x}\sin\pi z + c.c\right],$$
$$T_0 = \frac{1}{\delta^2}\left[Ae^{iq_{sc}x}\sin\pi z + c.c\right],$$
$$\phi_0 = \frac{-Na}{\delta^2}\left[Ae^{iq_{sc}x}\sin\pi z + c.c\right] \quad (38)$$

Where,

$$\begin{cases} A = A(X, Y, Z, T) - \ amplitude\ , \\ c.c. - complex\ \ conjugate\ . \end{cases}$$

We now scale the slow variables $(X, Y, Z, \& T)$ are as follows,

$$X = \epsilon x, \quad Y = \epsilon^{\frac{1}{2}} y, \quad Z = z, \quad T = \epsilon^2 t,$$

Using the these scaling, the differential operators may written in the following form,

$$\frac{\partial}{\partial x} \to \frac{\partial}{\partial x} + \epsilon\frac{\partial}{\partial X} \quad , \quad \frac{\partial}{\partial y} \to \frac{\partial}{\partial y} + \epsilon^{\frac{1}{2}}\frac{\partial}{\partial Y},$$
$$\frac{\partial}{\partial z} \to \frac{\partial}{\partial Z} \quad , \quad \frac{\partial}{\partial t} \to \epsilon^2\frac{\partial}{\partial T}. \quad (39)$$

By using Eq. (39), the operators L and N of Eq. (36) can be written as,

$$L = L_0 + \epsilon L_1 + \epsilon^2 L_2 \cdots,$$
$$N = N_0 + \epsilon N_1 + \epsilon^2 N_2 \cdots. \quad (40)$$

On substituting Eq. (40) into Eq. (36), and comparing the coefficients of ϵ, ϵ^2 and ϵ^3, one obtains,

$$L_0 w_0 = 0, \quad (41)$$
$$L_0 w_1 + L_1 w_0 = N_0, \quad (42)$$
$$L_0 w_2 + L_1 w_1 + L_2 w_0 = N_1. \quad (43)$$

where ,

$$L_0 = \frac{1}{Le}\nabla_h^2\nabla^2(Ra + NaRn)(Ha^2 + \nabla^2(1 + \frac{1}{\beta})) + \frac{1}{Le}Ha^2\nabla^4 D^2\left(Ha^2 - \nabla^2(1 + \frac{1}{\beta})\right)$$
$$-\frac{1}{Le}Ha^2\nabla^8(1 + \frac{1}{\beta}) + \frac{1}{Le}\nabla^{10}\left(1 + \frac{1}{\beta^2} + \frac{2}{\beta}\right) - \frac{1}{Le}\nabla^4 S_h^2 D^2(\nabla_h^2 - D^2), \quad (44)$$

$$L_1 = [(\frac{1}{Le}Ha^2(Ra + NaRn))(\nabla_h^2 + \nabla^2) - (\frac{1}{Le}Ha^2(1 + \frac{1}{\beta})(RnNa + Ra)(\nabla^2 - 2\nabla_h^2))$$
$$-\frac{1}{Le}Ha^2\nabla^4(1 + \frac{1}{\beta})(4\nabla^2 + 3D^2) + \frac{5}{Le}\nabla^8\left(1 + \frac{1}{\beta^2} + \frac{1}{\beta}\right)$$
$$+\frac{2}{Le}\nabla_h^2 S_h^2\nabla^2\left(D^2\nabla_h^2 - \frac{\nabla^2}{2} - 1\right)](((2\frac{\partial^2}{\partial x\partial X})^2),$$

$$L_2 = [\frac{1}{Le}Ha^4 D + \frac{1}{Le}(Ra + NaRn)\left(Ha^4 D - (1 + \frac{1}{\beta})(\nabla_h^2 - 2\nabla^2)\right) - \frac{1}{Le}Ha^2(1 + \frac{1}{\beta})\nabla^2(\nabla^2 + 3D) -$$
$$\frac{1}{Le}S_h^2 D^2((\nabla_h^2 - D^2) - 2\nabla^2)](((2\frac{\partial^2}{\partial x\partial X})^2) + [-\nabla_h^2 Ha^2 Ra - Ha^4 D\nabla^2(1 + \frac{1}{Le}) + \nabla_h^2 Ra\nabla^2(1 + \frac{1}{LePr} + \frac{1}{\beta}) +$$
$$\nabla_h^2\nabla^2\left(\frac{NaRn}{LePr} + \frac{Ra}{\beta}\right) + Ha^2\nabla^4\left(1 + \frac{1}{Le}(1 + \frac{1}{Pr}) + \frac{1}{\beta}(1 + \frac{1}{Le})\right)(D^2 + \nabla^2) - \nabla^8\left(1 + \frac{1}{Le}(1 + \frac{2}{Pr}) + \frac{1}{\beta^2}(1 + \frac{1}{Le}) +$$
$$\frac{2}{\beta} + \frac{2}{Le\beta}(1 + \frac{1}{Pr})\right) + S_h^2 D^2(\nabla_h^2 - D^2 + (1 + \frac{1}{Le})\nabla^2)](\frac{\partial}{\partial T}) + [\frac{1}{Le}Ha^2(Ra + NaRn)(\nabla_h^2 + \nabla^2) - \frac{2}{Le}\nabla^2\nabla_h^2\left((1 +$$
$$\frac{1}{\beta})(Ra + NaRn)\right) + \frac{2}{Le}Ha^4 D\nabla^2 - \frac{1}{Le}\nabla^4(1 + \frac{1}{\beta})\left(3Ha^2\frac{\partial}{\partial z} + Ra + NaRn\right) - \frac{4}{Le}Ha^2\nabla^6(1 + \frac{1}{\beta}) + \frac{5}{Le}\nabla^8\left(1 +$$
$$\frac{1}{\beta^2} + \frac{2}{\beta}\right) - \frac{1}{Le}S_h^2 D^2\nabla^2(2\nabla_h^2 - 2D^2 + 1)](\frac{\partial^2}{\partial X^2}). \quad (45)$$

Let us substitute the solution w_0 into $L_0 w_0 = 0$ and one obtains,

$$Ra_{sc} = -NaRn + \frac{Ha^2\pi^2\delta^2}{q^2} + \frac{(1+\frac{1}{\beta})\delta^6}{q^2} + \frac{\pi^2(-\pi^2+q^2)\delta^2 S_h^2}{q^2(Ha^2+(1+\frac{1}{\beta})\delta^2)}. \quad (46)$$

On substituting (38) in $L_0 w_1 + L_1 w_0 = N_0$, we get $N_0 = 0$ and $L_1 w_0 = 0$. The equation reduces to,

$$w_1 = 0, \quad (47)$$

$$u_1 = 0, \quad (48)$$

$$T_1 = \frac{-1}{2\pi\delta^2}|A|^2 sin2\pi z, \quad (49)$$

$$\phi_1 = \frac{NaLe}{2\pi\delta^2}(\frac{1}{Le} + 1)|A|^2 sin2\pi z. \quad (50)$$

On substituting these solutions in Eq. (43) , we obtain the Newell-Whitehead equation in the form of,

$$\lambda_0\frac{\partial A}{\partial T} - \lambda_1\left(\frac{\partial}{\partial X} - \frac{i}{2q}\frac{\partial^2}{\partial Y^2}\right)^2 A - \lambda_2 A + \lambda_3|A|^2 A = 0 \quad (51)$$

Where,

$$\lambda_0 = q^2 Ha^2 Ra - (1 + \frac{1}{Le})Ha^4\pi^2\delta^2 + \left(1 + \frac{1}{LePr}(1 + NaRn) + \frac{1}{\beta}\right)Raq^2\delta^2$$
$$-Ha^2\delta^4\left(1 + \frac{1}{LePr} + \frac{1}{\beta} + \frac{1}{Le} + \frac{1}{Le\beta}\right)(\pi^2 + \delta^2) - (1 + \frac{1}{Le})S_h^2\pi^2\delta^2(q^2 - \pi^2)$$
$$-\left(1 + \frac{1}{Le}\left(1 + \frac{2}{Pr}\right) + \frac{1}{\beta^2}\left(1 + \frac{1}{Le}\right) + \frac{2}{\beta} + \frac{2}{Le\beta}\left(1 + \frac{1}{Pr}\right)\right)\delta^8,$$

$$\lambda_1 = \left(\frac{Ha^2}{Le} + \frac{q^2}{Le}(1 + \frac{1}{\beta}) + \frac{2}{Le}\delta^2(1 + \frac{1}{\beta})\right)(Ra + NaRn) - \frac{Ha^2\pi^2}{Le}\left(Ha^2 + 3\delta^2(1 + \frac{1}{\beta})\right)$$
$$-\frac{6Ha^2\delta^4}{Le}(1 + \frac{1}{\beta}) - \frac{10}{Le}\delta^6\left(1 + \frac{2}{\beta} + \frac{1}{\beta^2}\right) + \frac{S_h^2\pi^2}{Le}(\pi^2 - q^2 - 2\delta^2 Le),$$

$$\lambda_2 = Raq^2\delta^2\left(Ha^2 + \frac{1}{Le}(1 + \frac{1}{\beta})\delta^2\right),$$

$$\lambda_3 = q^2\left((1 + \frac{1}{\beta})\delta^2 + Ha^2\right)\left(\frac{Ra}{2Le} + \frac{NaRn}{2Le} + \pi NaLeRn(1 + \frac{1}{Le})\right).$$

Considering only the x-dependence terms in Eq. (51), one obtains,

$$\frac{d^2A}{dX^2} + \frac{\lambda_2}{\lambda_1}\left(1 - \frac{\lambda_3}{\lambda_1}|A|^2\right)A = 0, \tag{52}$$

$$\therefore A(X) = A_0 tanh\left(\frac{X}{\wedge_0}\right). \tag{53}$$

Where, $\begin{cases} A_0 = \left(\frac{\lambda_2}{\lambda_3}\right)^{\frac{1}{2}}, \\ \wedge_0 = \left(\frac{2\lambda_1}{\lambda_2}\right)^{\frac{1}{2}}. \end{cases}$

6. Heat transport by convection

From Eq. (53), we get the maximum of steady amplitude ($|A_{max}|$) as,

$$|A_{max}| = (\frac{\epsilon^2\lambda_2}{\lambda_3})^{\frac{1}{2}} \tag{54}$$

We define Nusselt number in terms of amplitude A as,

$$Nu = 1 + \frac{\epsilon^2}{\delta_{Sc}^2}|A_{max}|^2, \tag{55}$$

From Eq. (55) , we obtain convection for $R > R_{T_{Sc}}$ and conduction for $R \leq R_{T_{Sc}}$. From Eq. (51), is valid for $\lambda_3 > 0$ which is possible when $R > R_{T_{Sc}}$, this we get,

1) convection for $Nu > 1$,

2) convection for $Nu \geq 1$(see in Fig.14).

7. Results and Discussions

This section presents a discussion of the results

Figure 2 illustrates the effect of the helical force parameter (S_h) on stationary convection, with other parameters (Rn, Na, β, Ha^2) held constant. The graph demonstrates that an increase in S_h results in a decrease in the critical Ra_{sc}, indicating that S_h exerts a destabilizing influence on the flow.

Figure 3 illustrates the impact on the critical Rayleigh number for various values of the nanoparticle Rayleigh number (Rn). The graph shows that as Rn increases, the critical Ra_{sc}, decreases, indicating that Rn has a destabilizing effect on the flow.

Figure 4 presents the neutral stability curves for the exchange of stabilities in the parametric plane (q,Ra_{sc}) for various values of the adjusted diffusivity proportion (Na), with fixed values of the nanoparticle Rayleigh number (Rn), Hartman number (Ha^2), ,Casson parameter(β) , helical force parameter (S_h) . The figure shows that as Na increases, the neutral stability curves shift downward monotonically, clearly indicating increased instability in the system. In other words, an increasing Na value has a destabilizing effect.

Figure 5 demonstrates how the stationary critical Rayleigh number of neutral curves are affected by the Hartman number (Ha^2). With other fixed numbers, the stationary critical Rayleigh number increases.This shows that as Ha^2 rises, the neutral stability curves shift monotonically increases, clearly indicating increased stability in the system. In other words, an increasing Ha^2 value has a stabilizing effect.

The impact of the Casson fluid parameter (β) on stationary instability is observed in figure 6.where increase in β leads to decrese in the critical Ra_{sc}.This establishes that when β grows, the temperature differential increases, resulting in a destabilizing effect of β. As a result, the system becomes less stable.

Figure 7 refers to the exchange of stabilities and displays neutral curves in the plane (q, Ra_{oc}) for different values of S_h. From this figure, one can observe that the neutral stability curves move downward monotonically as S_h increases, i.e., an increase in the S_h causes a destabilization in the system.

Figure 8 depicts the neutral curves for different values of Ha^2 at the onset of oscillatory convection, and it is found that the neutral curves move upward with an increase in the value ofHa^2, thus Ha^2 stabilizes the oscillatory convection.

Figure 9 illustrates the impact of the adjusted diffusivity ratio (Na) on the oscillatory critical Rayleigh number, an increase in Na leads to a decrease in the oscillatory critical Rayleigh number. This implies that as Na rises, which amplifies Na's destabilizing effect. As a result, the system's stability decreases.

Figure 10 depicts the effect of nanoparticle Rayleigh number (Rn) on the oscillatory instability, where it is observed that an increase in Rn leads to a decrease in the critical Ra_{oc}.This behavior can be explained by the fact that an increase in Rn leads to a decrease in the fluid flow, which enhances the instability.

Figure 11 shows that the effect of the Casson fluid parameter (β) on the oscillatory critical Rayleigh number . An increase in β leads to a increase in the oscillatory critical Rayleigh number. This indicates that as β increases, which enhancing β's stabilizing effect. Consequently, the system becomes more stable.

Figure 12 illustrates the influence of the Prandtl number (Pr) on the oscillatory critical Rayleigh number in the context of steady-state instability. From figure one can understand that an increase in Pr leads to a rise in the oscillatory critical Rayleigh number. This suggests that as Pr increases, thereby enhancing the stabilizing effect of Pr. As a result, the system becomes more stable.

Figure 13 presents the neutral curves for the exchange of stabilities in the parametric plane (q,Ra_{oc}) for various values of the Lewis number (Le), with fixed values of the nanoparticle Rayleigh number (Rn), Hartman number (Ha^2), Casson parameter(β), adjusted diffusivity ratio (Na) ,helical force parameter (S_h) and the Prandtl number (Pr) . The figure shows that as Le increases, the neutral stability curves shift upward monotonically, clearly indicating increased stability in the system. In other words, an increasing Le value has a stabilizing effect.

8. Conclusions

The paper investigates the thermal convection of a Casson fluid in a horizontal layer influenced by magnetic and helical force parameters. Both linear and weakly non-linear analyses are performed to assess the fluid's stability. The critical Rayleigh number is calculated in the linear analysis, while the Nusselt number is determined in the weakly non-linear analysis.A one-term Galerkin approach is employed to study the linear theory, while multiple scale analysis is used to investigate the weakly non-linear theory.

• The Hartman number (Ha) exerts a stabilizing effect on the system in both stationary and oscillatory convection.

• Meanwhile, the helical force parameter(S_h),the adjusted diffusivity ratio (Na), and the nanoparticle Rayleigh number (Rn) have a destabilizing effect on the system in both stationary and oscillatory convection.

• The Lewis number (Le) and Prandtl number(Pr) exhibit a stabilizing effect on oscillatory convection, but in the case of stationary convection, they do not have any impact on the system.

• The Casson parameter (β) has a destabilizing effect in the case of stationary convection, whereas it shows a stabilizing effect on the system in oscillatory convection.

References

[1] M. S. Aghighi, A. Ammar, C. Metivier, M. Gharagozlu (2018), Int. J. Therm. sci. 127, pp.79-90.
[2] M. Aneja, A. Chandra, S. Sharma (2020), Natural Convection in a Partially Heated Porous Cavity to Casson Fluid, Int. Comm. Heat Mass Transf. 114 1045555.
[3] J. Buongiorno, W. Hu (2005), Nanofluid coolants for advanced nuclear power plants, Paper no. 5705.In Proceedings of ICAPP '05, Seoul.
[4] S. Chakravarthy, S. Sarifuddin, P. K. Mandal (2004), Unsteady flow of a two-layer blood stream past a tapered flexible artery under stenotic conditions, Comput. Meth Appl Math, 4:391–409.
[5] S. Chandrasekhar (2013), Hydrodynamic and hydromagnetic stability, Courier Corporation.

[6] S. Choi (1995), Enhancing thermal conductivity of fluids with nanoparticles In: Siginer D.A., Wang, H.P. (eds.).
[7] A. L. Copley (1960), Apparent Viscosity and Wall Adherence of Blood Systems, In Flow Properties of Blood and Other Biological Systems, 97-121.
[8] M. Essoun and J. B. C. Orou (2012), Helical force effects on the onset of Küppers-Lortz instability with free-free Boundaries, Applied Physics Research, 4(3), 61.
[9] U. Gupta, J. Sharma, M. Devi (2020), Casson Nanofluid Convection in an Internally Heated Layer Mater, Today Proc. 28 1748-52.
[10] U. Gupta, J. Sharma, M. Devi (2021), Double-Diffusive Instability of Casson Nanofluids with Numerical Investigations for Blood-Based Fluid, Eur. Phys. J. Spec. Top. 9 (2021), https://doi.org/1.1140/epjst/s11734-021- 00053.
[11] M. Hamid, M. Usman, Z. H. Khan, R. Ahmad, W. Wang (2019), Dual Solutions and Stability of Flow and Heat Transfer of Casson Fluid Over a Stretching Sheet, Phys. Lett. A. 383 2400-2408.
[12] Madhy, Aneja, Avanish chandra, sapna sharma ((2020)), Int. commun. Heat mass transf.114, 104555.
[13] S. Mehmood, M. Nawaz and A. Ali (2018), Finite Volume Solution of Non-Newtonian Casson Fluid Flow in A Square Cavity, Communications in Mathematics and Applications, 9(3), 459.
[14] M. Mustafa, T. Hayat, I. Pop and A. Aziz (2011), Unsteady boundary layer flow of a Casson fluid due to an impulsively started moving flat plate, Heat Transfer Asian Research, 40(6), 563-576.
[15] D. A. Nield, A. V. Kuznetsov (2009), The onset of convection in a nanofluid layer, ASME J. Heat Transf.
[16] D. A. Nield, A. V. Kuznetsov (2010), The Onset of Convection in a Horizontal Nanofluid Layer of Finite Depth Euro, J. Mech. B/Fluids, 29 217-223.
[17] G. Pomalègni, M. Essoun, A. V. Kpadonou, J. B. CHABI OROU (2014), Effects of Magnetic Field and Helical Force on the Onset of Rayleigh-Bénard Convection with Free-Free Boundaries, The African Review of Physics, 9.
[18] G. S. K. Reddy and R. Ragoju (2022), Thermal instability of a power-law fluid-saturated porous layer with an internal heat source and vertical throughflow, Heat Transfer, 51(2), 2181-2200.
[19] G. W. Scott Blair (1959), An Equation for the Flow of Blood Plasma and Serum Through Capillaries Nature, 183 613-614.
[20] G. W. Scott Blair (1966), The Success of Casson's Equation Rheo, Acta Sep. 5(3) 184-187.
[21] J. F. Steffe (1996), Rheological methods in food process engineering, Freeman press.
[22] D. Y. Tzou (2008), Instability of Nanofluids in Natural Convection, ASME J. Heat Trans. 130 1-9.
[23] D. Y. Tzou (2008), Thermal Instability of Nanofluids in Natural Convection, Int. J. Heat Mass Transf., 51 2967-79.
[24] D. Yadav, G. S. Agrawal, R. Bhargava (2011), Rayleigh-Benard Convection in Nanofluid, Int J. Appl. Math. Mech. 7(2) 61-76.